Subnanosecond $KTiOPO_4$ optical parametric oscillator intracavity pumped by a Kerr-lens, mode-locked YVO_4/Nd:YVO_4 laser coupled with an acousto-optic modulator

Hongwei Chu, Jia Zhao, Kejian Yang, Shengzhi Zhao,* Tao Li, Dechun Li, Guiqiu Li, and Wenchao Qiao

School of Information Science and Engineering, Shandong University, Jinan 250100, China
**Corresponding author: shengzhi_zhao@sdu.edu.cn*

Received June 22, 2015; revised July 27, 2015; accepted July 27, 2015;
posted July 29, 2015 (Doc. ID 243524); published September 10, 2015

A Kerr-lens, mode-locked YVO_4/Nd:YVO_4 laser coupled with an acousto-optic modulator (AOM) *Q*-switching near 1064 nm was employed to pump an intracavity $KTiOPO_4$ (KTP) optical parametric oscillator. A subnanosecond signal wave near 1572 nm with low repetition rate was realized. At an AOM repetition rate of 8 kHz, the maximum output power was 165 mW. The highest average pulse energy, the shortest duration, and the highest peak power of a mode-locking signal pulse were estimated to be ~10.3 μJ, ~120 ps, and ~82 kW, respectively.

OCIS codes: (190.4410) Nonlinear optics, parametric processes; (140.7090) Ultrafast lasers; (190.3270) Kerr effect.
http://dx.doi.org/10.1364/PRJ.3.000260

1. INTRODUCTION

Because of their excellent physicochemical, optical, and mechanical properties, such as wide absorption bandwidths at 808 nm (~21 nm), high absorption coefficients, and large stimulated emission cross sections, Nd:YVO_4 crystals have been extensively employed as laser media in continuous wave, *Q*-switching, and mode-locking operations [1–3]. However, owing to their small thermal conductivity, Nd:YVO_4 crystals suffer from serious thermal effects at high pump powers, which limits the output laser characteristics. Previous experimental results have shown that it can efficiently abate thermal effects in the composite YVO_4/Nd:YVO_4 crystal by using the thermal diffusion-bonding technique [4–6]. Moreover, YVO_4 crystal possesses a high third-order nonlinearity $\chi^{(3)}$, which is closely related to the stimulated Raman scattering (SRS) process and the Kerr-lensing effect. Therefore, the composite YVO_4/Nd:YVO_4 crystal is expected to have excellent performance in either self-Raman or Kerr-lens, mode-locking (KLM) operations. Many papers have reported on the SRS process in Nd:YVO_4 composite crystal [7,8]. With respect to the KLM operation, because they can produce ultrashort pulses in the scale of femtoseconds (fs) without any other optical elements in the resonator [9], KLM lasers have found a vast number of applications in scientific research fields such as optical sensing, material processing, and nonlinear optics, especially in the generation of terahertz radiation. To date, Nd:YVO_4 single crystal has been exploited to realize self-starting KLM operation [10,11], elucidating the large third-order nonlinear optical response of YVO_4 crystal.

In order to generate ultrafast pulses with high peak power and large pulse energy, the mode-locking operation is generally combined with the actively *Q*-switching operation, which is called simultaneous *Q*-switching and mode locking (QML). In those QML lasers, the envelope repetition rate is exactly controlled by the external signal. Thus, stable envelope trains with low repetition rates and high energy can be easily realized. The first KLM operation coupled with the *Q*-switching technology is accomplished by simultaneously using two acousto-optic modulators (AOMs) in a cavity [12]. Subsequently, by employing one AOM, a KLM Nd:YAG green laser was also realized [13]. Recently, combining the KLM operation and the AOM *Q*-switching operation, a self-Raman YVO_4/Nd:YVO_4/YVO_4 laser was demonstrated with a mode-locked pulse duration of about 24 ps [14].

Optical parametric oscillators (OPOs), another common nonlinear frequency conversion technology, can generate tunable sources with wide spectral ranges. For the ps signal pulses, most conventional OPOs adopt extracavity pumping configurations by continuous wave mode-locked lasers. In order to obtain high peak power and pulse energy, one can reduce the pulse repetition rate. Pumped by using a low-repetition-rate, Yb:fiber-amplified, gain-switched ps laser diode, an extracavity OPO with the cavity length of 42 m and repetition rate of 7.19 MHz was reported [15]. However, the pulse energy of the signal wave was estimated to be only about 0.49 μJ. One breakthrough in extracavity OPO operation has been made by employing a low-repetition-rate QML laser as a pump source [16]. However, the laser system suffered from large size, bulkiness, and complexity. It is well known that the pulse duration of the signal wave from an intracavity OPO (IOPO) can be shortened in comparison with that of the fundamental wave [17]. Meanwhile, the intracavity power is higher than the output power and can undergo multiple passes through the nonlinear optical crystal. Therefore, the IOPO operation seems more suitable for high-peak-power single-pulse generation. For the intracavity ps OPO with low repetition rate, a dual-loss modulated QML Nd:GGG/KTiOPO$_4$ (KTP) IOPO has been realized with a pulse duration of 290 ps and a peak power of 15.9 kW [18]. Recently, we have realized a KTP IOPO pumped by a KLM Nd:GGG laser coupled with a single AOM [19]. The experimental results demonstrated that the KLM laser pump IOPO is feasible. However, owing to the low third-order nonlinearity of Nd:GGG, the mode-locking characteristics of the fundamental and the signal waves were still poor.

In this paper, we developed a KTP IOPO pumped by a KLM YVO$_4$/Nd:YVO$_4$ laser coupled with an AOM Q-switching operation. With an AOM repetition rate of 8 kHz, a maximum output power of 165 mW was achieved under an incident diode pump power of 8.25 W. The shortest duration and the highest peak power of each signal pulse were estimated to be about 120 ps and 82 kW, respectively.

2. EXPERIMENTAL SETUP

Figure 1 shows the schematic configuration of the KTP OPO intracavity pumped by a KLM YVO$_4$/Nd:YVO$_4$ laser coupled with an AOM Q-switching operation. The pump source was a fiber-coupled laser diode (FAP-I system, Coherent Inc., USA) with a central wavelength at 808 nm. The core diameter and the numerical aperture of the coupled fiber were 400 μm and 0.22, respectively. The pump beam was collimated and focused into the composite crystal by an optics system (1:1 imaging module). The input mirror M_1 was a plane mirror with a high-reflectivity (HR) coating at 1064 nm ($R > 99.5\%$) and high-transmission (HT) coating at 808 nm ($T = 85\%$). The folded mirror M_2 was a concave mirror with a radius of curvature of 200 mm and HR coating at 1064 nm ($R > 99.8\%$). The output coupler (OC) was a plane mirror with a transmission of $T = 4\%$ at 1570 nm and HR coating at 1064 nm ($R > 99.5\%$). The composite crystal YVO$_4$/Nd:YVO$_4$ was grown by thermal diffusion technology with dimensions of $4\ \text{mm} \times 4\ \text{mm} \times (3 + 8)$ mm. Nd:YVO$_4$ crystal was cut along the a axis and had a dopant concentration of 1 at.%. An X-cut ($\theta = 90°$, $\phi = 0°$) KTP crystal with dimensions of $5\ \text{mm} \times 5\ \text{mm} \times 20$ mm was used for Type-II noncritical phase matching in order to eliminate the walk-off effect and hold a maximum effective nonlinear coefficient. The input surface of the KTP crystal was HR coated at a range from 1500 to 1600 nm ($R > 99.8\%$) and AR coated at 1064 nm ($R < 0.2\%$), while the other surface was AR coated at both spectral ranges ($R < 0.5\%$). Both the laser crystal YVO$_4$/Nd:YVO$_4$ and the nonlinear crystal KTP were wrapped with a thin layer of indium foil and mounted in copper holders maintained at 18°C. A 47 mm long AOM GSQ27-3 (26th Institute, CETC, China) with AR coatings at 1064 nm ($R < 0.2\%$) on both surfaces was employed as the active Q-switch in the experiment. The presented fundamental wave configuration was a V-type cavity with a physical length of about 395 mm (corresponding to an optical length ~435.1 mm). The output power was measured by a MAX 500AD laser power meter (Coherent Inc., USA), and the temporal pulse characteristics were recorded by a DPO 7104C digital phosphor oscilloscope (1 GHz bandwidth, Tektronix Inc., USA) via a fast InGaAs photo detector with a rising time of about 400 ps (model 1611, Newport Inc., USA). The spectra were measured by a WaveScan Laser spectrometer with a resolution of 0.4 nm (APE GmbH, Germany).

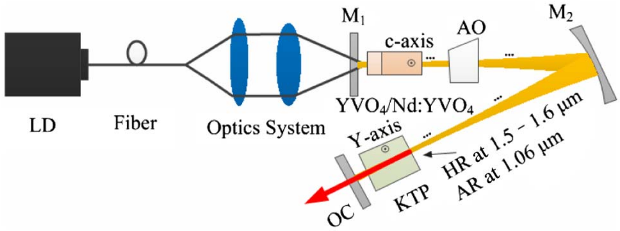

Fig. 1. Schematic setup of the intracavity KTP OPO pumped by a KLM YVO$_4$/Nd:YVO$_4$ laser coupled with an AOM.

3. RESULTS AND DISCUSSION

We first investigated the KLM YVO$_4$/Nd:YVO$_4$ laser without KTP crystal. In this case, another OC with a transmission of $T = 6.5\%$ at 1064 nm was employed. Considering the thermal effect in the composite crystal and the ABCD matrix for a beam via a Kerr element, the Gaussian beam waist w in the resonator can be calculated. The parameter δ is defined to describe the saturable absorption [13]:

$$\delta = \frac{1}{w}\frac{dw}{dp}\Big|_{p=0}, \tag{1}$$

where p is the ratio of the intracavity power to the critical power for self-focusing. When the parameter δ is negative and big enough in modulus, the KLM operation can be realized. Under an incident pump power of 8.76 W, δ was (−1.64) according to our calculation. Therefore, a KLM YVO$_4$/Nd:YVO$_4$ laser could be expected. The maximum output power of about 1.28 W for the KLM YVO$_4$/Nd:YVO$_4$ laser coupled with an AOM was obtained at a repetition rate of 8 kHz and an incident pump power of 8.76 W. A typical Q-switched envelope is shown in Fig. 2. As shown in Fig. 2(a), the modulation depth of a KLM YVO$_4$/Nd:YVO$_4$ laser is about 90%. The separated time of the neighbor mode-locking pulses was about 2.9 ns, which accorded well with the round-trip time in the cavity. As shown in Fig. 2(b), there are harmonic mode-locking pulses underneath the Q-switched envelope.

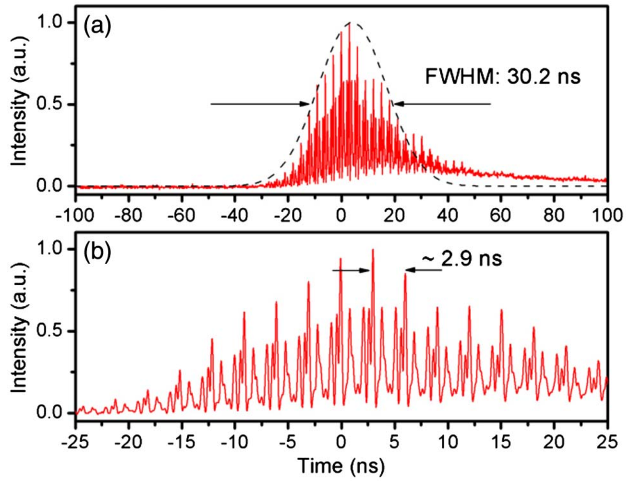

Fig. 2. Typical pulse trace with an AOM under incident pump power of 8.76 W. (a) KLM laser, (b) expanded pulse trace. Dashed line: Gaussian fitting.

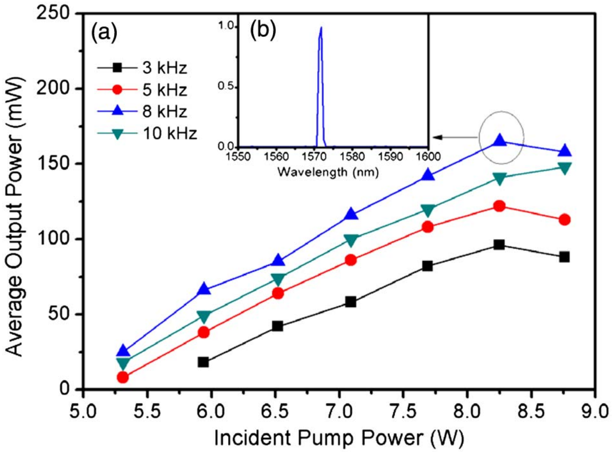

Fig. 3. Average output power of signal wave versus incident pump power. Inset: typical spectra.

Therefore, the average output power and peak power of each mode-locking pulse would decrease abruptly.

After a KTP crystal was inserted into the laser cavity, as discussed in detail in [18], when the distance between the output surface of KTP and OC was about 5 mm, corresponding to the OPO cavity length of approximately 25 mm, the signal wave can be generated. The average output power is shown in Fig. 3(a). In order to generate high pulse energy, the AOM repetition rate varied from 3 to 10 kHz. Owing to the low Q-switching efficiency and large losses in the resonator, the threshold diode pump power was about 5.94 W with the AOM repetition rate at 3 kHz. From Fig. 3, a maximum output power of 165 mW is obtained with a repetition rate of 8 kHz under an incident pump power of 8.25 W, corresponding to an optical-to-optical conversion efficiency of 2%. At an AOM repetition rate of 10 kHz, although the number of the Q-switched envelope at unit time increased, the pulse energy per Q-switched envelope decreased, which may be predominant for the generation of the IOPO [20]. Therefore, a lot of attention was paid to the AOM repetition rate of 8 kHz. We believed that the conversion efficiency could be further increased with a shorter nonlinear crystal with high nonlinear coefficient d_{eff} to reduce the group velocity dispersion. However, there are no other nonlinear crystals available in our lab. The inset Fig. 3(b) shows the typical spectra at an incident diode pump power of 8.25 W with an AOM repetition rate of 8 kHz. The intense peak near 1572 nm was the signal wavelength, which fitted well with the noncritical phase-matching (NCPM) condition of the KTP crystal. The idler wave (~3.3 μm, calculated wavelength) is difficult for us to measure, owing to the limitations of the spectrometer employed in our experiment, the absorption of OC (made by K9 glass), and the nonlinear optical crystal.

A dichroic mirror with HR coating at 1064 nm and HT coating at 1570 nm was placed behind the OC. The temporal pulse behaviors of the signal beam and the depleted fundamental beam were recorded by the digital oscilloscope. Figure 4 shows the depleted fundamental wave and the signal wave under an incident pump power of 5.94 W. From Fig. 4, one can easily see that the modulation depth of the signal wave reaches nearly 100%. The interval time of the mode-locking pulses underneath a Q-switched envelope was about 2.9 ns, which accorded well with the round-trip time.

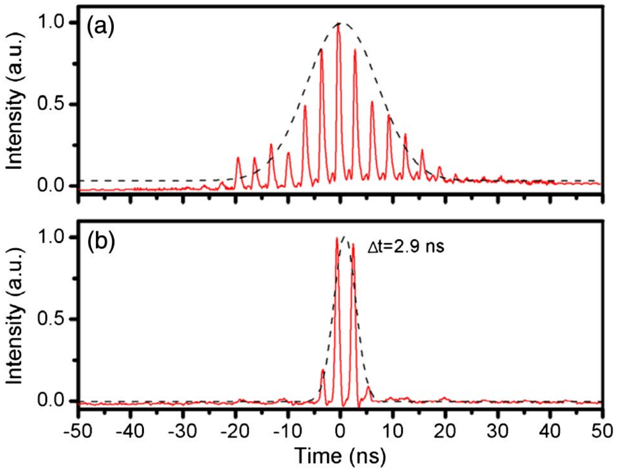

Fig. 4. (a) Depleted fundamental wave and (b) signal wave at pump power of 5.94 W. Dashed lines: Gaussian fittings.

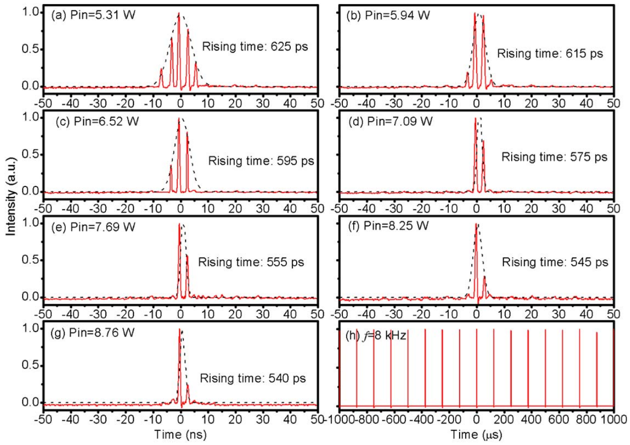

Fig. 5. Typical pulse traces of the signal wave versus incident pump power. Pin: incident pump power. (a) 5.31, (b) 5.94, (c) 6.52, (d) 7.09, (e) 7.69, (f) 8.25, (g) 8.76 W. Dashed lines: Gaussian fittings. (h) $f = 8$ MHz.

Figure 5 shows the typical pulse shapes under different incident pump power. As shown in Fig. 5(a), there are five mode-locking pulses underneath the Q-switched envelope at an incident pump power of 5.31 W. With the increase of the incident pump power, the number of the mode-locking pulses underneath a Q-switched envelope decreased. Moreover, according to the Gaussian fitting of the Q-switched envelope, the Q-switched envelope duration decreased from about 8.7 ns under an incident pump power of 5.31 W to about 2.2 ns under an incident pump power of 8.76 W. A typical pulse train of the signal wave is given in Fig. 5(h), demonstrating the stable QML OPO operation. According to the pulse train, the pulse-to-pulse amplitude fluctuations of the signal wave were smaller than 3%. To theoretically explain the variations of the temporal shapes, we used the deduced coupled rate equations describing the IOPO operation pumped by a KLM laser in [19]. The corresponding temporal profiles at different incident pump powers are illustrated in Fig. 6.

For QML pulses, the real rising time of the mode-locking pulse duration can be evaluated by the rising time of the

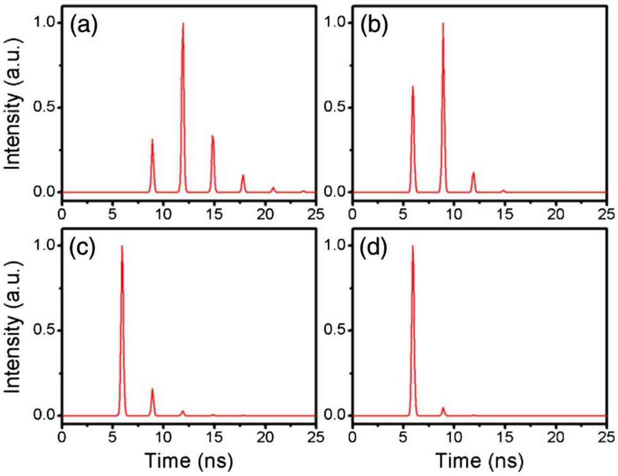

Fig. 6. Theoretical temporal profiles at incident pump power (a) 5.31, (b) 6.52, (c) 7.69, and (d) 8.76 W.

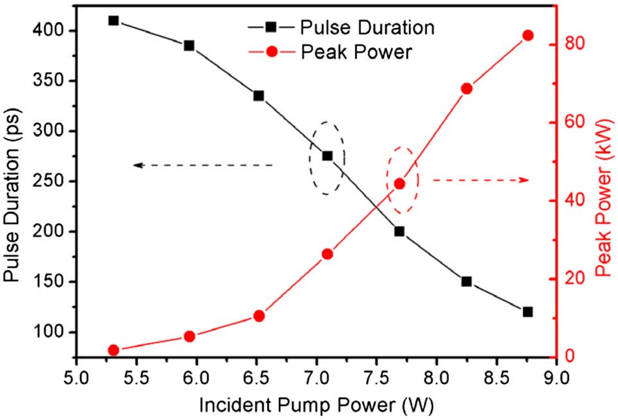

Fig. 7. Pulse duration and peak power versus incident pump power.

mode-locking pulses, the photo detector, and the oscilloscope [21]. The measured rising time of the mode-locking pulses can be seen in Fig. 5. Figure 7 shows the mode-locking pulse duration versus the incident pump power. According to the relationship of the average output power, the modulation rate, the pulse duration, and the number of the mode-locking pulse underneath a Q-switched envelope, the average pulse energy of each mode-locking pulse can be calculated. At an incident pump power of 8.25 W, considering there are two mode-locking pulses underneath the Q-switched envelop, the maximum average pulse energy for each mode-locking pulse was ~10.3 μJ. The average peak power of each mode-locking pulse is shown in Fig. 7. From Fig. 7, the minimum mode-locking pulse duration is approximately 120 ps, while the highest peak power is about 82 kW. M^2 factors of the signal beam were measured to be smaller than 1.5 by using the knife-edge method.

4. CONCLUSIONS

In conclusion, an intracavity KTP OPO pumped by a KLM $YVO_4/Nd:YVO_4$ laser coupled with an AOM was realized. The signal wave could be obtained with a maximum output power of 165 mW. The shortest mode-locking pulse duration was estimated to be 120 ps, corresponding to a highest peak power of about 82 kW.

Acknowledgment

This work is partially supported by the National Natural Science Foundation of China (61378022), the National Natural Science Foundation of China for Youths (61205145), the Fundamental Research Funds of Shandong University (2014JC032), the China Postdoctoral Science Foundation (2013M541901), and Independent Innovation Foundation of Shandong University, IIFSDU (2013HW013 and 2014TB011).

REFERENCES

1. R. Conroy, T. Lake, G. Friel, A. Kemp, and B. Sinclair, “Self-Q-switched Nd:YVO_4 microchip lasers,” Opt. Lett. **23**, 457–459 (1998).
2. Y. Chen, S. Tsai, and S. Wang, “High-power diode-pumped Q-switched and mode-locked Nd:YVO_4 laser with a Cr^{4+}:YAG saturable absorber,” Opt. Lett. **25**, 1442–1444 (2000).
3. P. Blandin, F. Druon, F. Balembois, P. Georges, S. Leveque-Fort, and M. Fontaine-Aupart, “Diode-pumped passively mode-locked Nd:YVO_4 laser at 914 nm,” Opt. Lett. **31**, 214–216 (2006).
4. M. Tsunekane, N. Taguchi, and H. Inaba, “High power operation of diode-end pumped Nd:YVO_4 laser using composite rod with undoped end,” Electron. Lett. **32**, 40–42 (1996).
5. T. Li, Z. Zhuo, X. Li, H. Yang, and Y. Zhang, “Study on optical characteristics of Nd:YVO_4/YVO_4 composite crystal laser,” Chin. Opt. Lett. **5**, 175–177 (2007).
6. Z. Zhuo, T. Li, X. Li, and H. Yang, “Investigation of Nd:YVO_4/YVO_4 composite crystal and its laser performance pumped by a fiber coupled diode laser,” Opt. Commun. **274**, 176–181 (2007).
7. Y. Chang, K. Su, H. Chang, and Y. Chen, “Compact efficient Q-switched eye-safe laser at 1525 nm with a double-end diffusion-bonded Nd:YVO_4 crystal as a self-Raman medium,” Opt. Express **17**, 4330–4335 (2009).
8. W. Chen, Y. Wei, C. Huang, X. Wang, H. Shen, S. Zhai, S. Xu, B. Li, Z. Chen, and G. Zhang, “Second-Stokes YVO_4/Nd:YVO_4/YVO_4 self-frequency Raman laser,” Opt. Lett. **37**, 1968–1970 (2012).
9. A. Lagatsky, A. Sarmani, C. Brown, W. Sibbett, V. Kisel, A. Selivanov, I. Denisov, A. Troshin, K. Yumashev, N. Kuleshov, V. Matrosov, T. Matrosova, and M. Kupchenko, “Yb^{3+}-doped YVO_4 crystal for efficient Kerr-lens mode locking in solid-state lasers,” Opt. Lett. **30**, 3234–3236 (2005).
10. H. Liang, C. Chen, Y. Huang, K. Su, and Y. Chen, “Compact efficient multi-GHz Kerr-lens mode-locked diode-pumped Nd:YVO_4 laser,” Opt. Express **16**, 21149–21154 (2008).
11. H. Liang, Y. Huang, W. Huang, K. Su, and Y. Chen, “High-power, diode-end-pumped, multigigahertz self-mode-locked Nd:YVO_4 laser at 1342 nm,” Opt. Lett. **35**, 4–6 (2010).
12. D. Kuizenga, “Short-pulse oscillator development for the Nd:glass laser-fusion systems,” IEEE J. Quantum Electron. **17**, 1694–1708 (1981).
13. V. Donin, D. Yakovin, and A. Gribanov, “Diode-pumped green Nd:YAG laser with Q-switch and mode locking,” Opt. Lett. **37**, 338–340 (2012).
14. G. Huang, Y. Yu, X. Xie, Y. Zhang, and C. Du, “Diode-pumped simultaneously Q-switched and mode-locked YVO_4/Nd:YVO_4/YVO_4 crystal self-Raman first-Stokes laser,” Opt. Express **21**, 19723–19731 (2013).
15. F. Kienle, P. Teh, S. Alam, C. Gawith, D. Hanna, D. Richardson, and D. Shepherd, “Compact, high-pulse-energy, picosecond optical parametric oscillator,” Opt. Lett. **35**, 3580–3582 (2010).
16. K. McEwan, “High-power synchronously pumped $AgGaS_2$ optical parametric oscillator,” Opt. Lett. **23**, 667–669 (1998).
17. Y. Chen, S. Chen, L. Tsai, Y. Chen, and C. Chien, “Efficient subnanosecond intracavity optical parametric oscillator pumped with a passively Q-switched Nd:$GdVO_4$ laser,” Appl. Phys. B **79**, 823–825 (2004).
18. H. Chu, S. Zhao, K. Yang, J. Zhao, Y. Li, D. Li, G. Li, T. Li, and W. Qiao, “Intracavity KTP-based OPO pumped by a dual-loss modulated, simultaneously Q-switched and mode-locked Nd:GGG laser,” Opt. Express **22**, 26925–26932 (2014).

19. H. Chu, S. Zhao, K. Yang, J. Zhao, Y. Li, T. Li, G. Li, D. Li, and W. Qiao, "Intracavity KTP optical parametric oscillator driven by a KLM Nd:GGG laser with a single AO modulator," Opt. Laser Technol. **68**, 73–78 (2015).
20. J. Yang, S. Liu, J. He, X. Yang, F. Liu, B. Zhang, J. Xu, H. Yang, and H. Huang, "Tunable simultaneous dual-wavelength laser at 1.9 and 1.7 μm based on $KTiOAsO_4$ optical parametric oscillator," Laser Phys. Lett. **8**, 28–31 (2011).
21. T. Li, S. Zhao, Z. Zhuo, K. Yang, G. Li, and D. Li, "Dual-loss-modulated Q-switched and mode-locked YVO_4/Nd:YVO_4/KTP green laser with EO and Cr^{4+}:YAG saturable absorber," Opt. Express **18**, 10315–10322 (2010).